Simulation of silicon thermal oxidation

Chongmu Lee
Department of Metallurgical Engineering, Inha University, Inchon 160, Korea
(Received 12 December 1986)

Thermal oxidation of silicon is simulated employing a potential-energy function composed of two- and three-body potentials. For convenience the simulation is performed for two separate oxidation process steps: the adsorption of oxygen atoms on the silicon substrate and the formation of a macroscopic oxide layer. The latter is implemented by simulating the silicon and silica blocks placed in contact. The simulation provides the atomic configurations of a clean silicon surface, oxygen-adsorbed silicon surfaces, and a Si-SiO_2 interface as well as binding energies for oxygen on silicon surfaces.

I. INTRODUCTION

In general, computer simulation provides us with atomic-level understanding which is very important for quantitative studies of the structure and properties of materials. Simulation of thermal oxidation of silicon (Si) will give us useful insight into atomic configuration and energetics near the Si surface and the Si-SiO_2 interface.

Thermal oxidation is the most widely used method for the preparation of Si-SiO_2 interfaces in commercial electronic devices. However, direct simulation of this method is not feasible, since too much simulation time would be required to attain equilibrium. Therefore, the simulation of thermal oxidation of Si was implemented by simulating two steps of the oxidation process separately. According to the experimental work[1] reported on the oxidation of Si surfaces, the exposure of clean Si surfaces to an oxygen atmosphere leads to different growth regimes of chemisorption. The first regime is a rapid process of chemisorption which continues until a saturation level is reached, corresponding to formation of it, at most, a few monolayers. The next regime is the slow formation of a macroscopic oxide layer [dominated by diffusion of oxygen (O) atoms through the oxide and reaction at the Si-SiO_2 interface].[2]

In this investigation, first, reconstruction of a clean Si surface will be discussed. Then adsorption of O atoms on the Si substrate (the first regime of thermal oxidation) will be considered. Finally simulations of the interface of Si and SiO_2 blocks placed in contact, which is equivalent to the second regime of thermal oxidation, will be discussed. This simulation was performed by placing crystalline Si and SiO_2 blocks together and allowing the regions near the interface to relax.

In many of the simulation methods which deal with discrete particles the semiempirical pair potentials have been employed to analyze energy and structure-related properties of the system. However, it is now well accepted that many-body interactions are required for a proper presentation of the total energy for many systems. In other words, noncentral force terms should be included in a potential-energy function (PEF) to calculate some important structures and properties of surfaces. In the early studies we developed a PEF including three-body interactions in addition to two-body interactions for the simulations of Si/O systems and parametrized the potentials so that many-body effects could be included into the PEF.

In the present study simulations were performed employing a Monte Carlo procedure and the same PEF as was used in the earlier studies.[3-5]

II. POTENTIAL-ENERGY FUNCTION

The total potential energy of a cluster with N atoms is calculated employing the following potential-energy function:[6,7]

$$\Phi=\frac{1}{2!}\sum_{i=1}^{N}\sum_{\substack{j=1\\(j\neq i)}}^{N}U(\gamma_i,\gamma_j)+\frac{1}{3!}\sum_{i=1}^{N}\sum_{\substack{j=1\\(j\neq i)}}^{N}\sum_{\substack{k=1\\(i\neq k\neq j)}}^{N}U(\gamma_i,\gamma_j,\gamma_k)\,, \tag{1}$$

where $U(\gamma_i,\gamma_j)$ and $U(\gamma_i,\gamma_j,\gamma_k)$ denote the two-body and three-body interactions between the atom i and its surroundings. The two-body part is represented by the Mie potential,

$$U(\gamma_{ij})=\frac{\epsilon}{(m-n)}\left[n\left[\frac{\gamma_0}{\gamma_{ij}}\right]^m-m\left[\frac{\gamma_0}{\gamma_{ij}}\right]^n\right], \tag{2}$$

where $\gamma_{ij}=|\gamma_i-\gamma_j|$; γ_0 represents the equilibrium distance and ϵ denotes the two-body energy at $\gamma_{ij}=\gamma_0$. The exponents m and n account for the repulsive and attractive terms, respectively. The three-body part, on the other hand, is represented by the Axilrod-Teller tripole-dipole potential,

$$U(\gamma_i,\gamma_j,\gamma_k)=\frac{Z(1+3\cos\theta_i\cos\theta_j\cos\theta_k)}{(\gamma_{ij},\gamma_{ik},\gamma_{jk})^3}\,, \tag{3}$$

where Z denotes the three-body intensity parameter. $\theta_i,\theta_j,\theta_k$ and $\gamma_{ij},\gamma_{ik},\gamma_{jk}$ represent the angles and the sides of the triangle formed by the three particles i, j, and k, respectively.

The values of the parameters for the above equations used in this simulation are given in Table I. These pa-

TABLE I. Potential-energy parameters (Ref. 5).

Two-body parameters	(Si-Si)	(O-O)	(Si-O)
(K)	37 745	59 943	47 355
(Å)	2.25	1.208	1.622

Three-body intensity parameters	(Si-Si-Si)	(O-O-O)	(Si-Si-O)	(Si-O-O)
Z (K Å)	61 361 332	262 682	5 659 026	4 485 348

rameters were recently calculated from fits to experimental data for materials involving Si and O atoms.[3] Here, we also set $m=12$ and $n=6$ which reduces the two-body part of the potential to a Lennard-Jones potential.

III. CALCULATIONAL PROCEDURE, RESULTS, AND DISCUSSION

A. Clean Si surface

The model system employed in this simulation is three lattice parameters long in the [100] and [010] directions and three atomic layers long in the [001] direction. This system was made semi-infinite in the [100] and [010] directions by imposing periodic boundary conditions. Thus the exposed surface is represented by a (001) plane. The cutoff radius was taken as 6.0 Å. All iterations in the Monte Carlo procedure were carried out until complete equilibration, which was monitored by the variation in the total potential energy of the system.

The top views of the clean Si(001) surface before and after relaxation are shown in Figs. 1(a) and 1(b). In these figures the solid-outlined, dashed-outlined, and dotted-outlined circles represent atoms in the first, second, and third layers from the surface, respectively.

Only the first layer was allowed to relax at 300 K in this simulation. The initial structure of the Si(001) surface displayed a (1×1) configuration, but the equilibrated surface exhibits a (2×2) or (1×1) pattern. This result is in good agreement with the experimental results where (2×1), (4×2), and (1×1) patterns were observed on Si(001) surfaces.[8,9] The reconstruction pattern for the Si(001) surface obtained in the present work is very similar to the (2×1) pattern obtained experimentally. Both patterns show the formation of dimers; however, dimers from alternately in the present work, while they are interpreted to form successively in the experiment.

B. O adsorption on the Si surface

There are some differences between an O atom and an O_2 molecule in the binding mode when they are chemisorbed on Si surfaces.[2] In the present study only the adsorption of O atoms will be considered.

What is the most favorable site for an O atom when it is adsorbed on the Si(001) surface? In order to find this out we put an O atom at several candidating positions and compared the total potential energies of the system after relaxation. We used the same model system for an initial Si substrate in this simulation as that used for the simulation of the clean Si surface. According to the simulation results the O adsorption site lies slightly above the midpoint between two Si atoms which approach each other through relaxation [position "A" in Figs. 1(a) and 1(b)]. This result agrees well with that obtained by Batra *et al.*[10] based on the cluster and slab calculations. They found that O in the first layer bridging positions is more stable

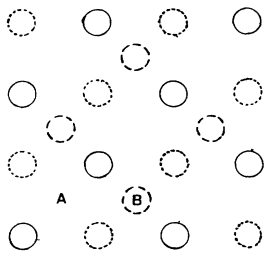

(a) UNRELAXED Si (001) SURFACE

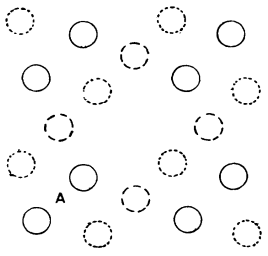

(b) RELAXED Si (001) SURFACE

FIG. 1. Top view of the atomic arrangement near the Si(001) surface: (a) before relaxation and (b) after relaxation. Solid-outlined, dashed-outlined, and dotted-outlined circles represent atoms belonging to the first, second, and third layers from the surface, respectively. The atoms of the first layer are numbered.

than in the on-top configuration and the fourfold center site. The adsorption or binding energy of one O atom on the Si(001) surface calculated from the total potential-energy difference is −8.4 eV.

When nine O atoms were adsorbed on the Si(001) surface in Fig. 1(a), all nine of the same type of absorption site as position *A* in this figure were saturated with O atoms. The average Si—O bond length for the system is 1.60 Å which is almost the same as that in the bulk SiO_2. This value is rather closer to 1.64 Å for the on-top site than to 1.92 Å for the bridging site calculated by Batra *et al.*[10] Other values reported for the Si—O bond length are 1.69 Å (by Goddard *et al.*[2] using *ab initio* calculation) and 1.65 Å (by Schaefer *et al.*[11] using electron-energy-loss spectroscopy and x-ray photoemission spectroscopy). The average Si—O—Si angle is 163° which is larger than that in the bulk (144°). Also this angle is much larger than 130° found by Schaefer *et al.*[11] for an O atom adsorbed on the Si(100) surface. The adsorption energy of nine O atoms into crystalline Si calculated in this simulation is −74.6 eV (see Table II). This is approximately nine times the adsorption energy for one O atom. This result is consistent with the adsorption energy presented above considering the error range due to the effect of thermal fluctuations. However, the value of 8.3 eV found in this work for the binding energy of O and Si is much larger than 4.28 eV calculated by Batra *et al.*[10] for an O atom in the bridge site on the Si(100) 1×1 surface. The values of the binding energy for O chemisorption on Si(100) and Si(111) surfaces reported by others[2,11–13] are in the range of 0.9–3.7 eV.

When nine more O atoms were deposited onto the Si surface with the first nine O adatoms already adsorbed, half of the second most energetically favorable positions [the positions of type *B* in Fig. 1(a)] were alternately occupied [Fig. 2(a)]. These nine O atoms of the second adlayer moved deeper inside than the first nine O adatoms. In other words, the first nine O adatoms in positions of type *A* were pushed upwards about 1 Å by the second nine adatoms. Thus they are distributed in the range from positions 10 to 11 [Fig. 2(b)], and the second nine adatoms are distributed about 1 Å lower, i.e., in the range of positions 9 to 10.

The adsorption energy for the second nine O adatoms is calculated to be 110.0 eV, which is approximately 1.5 times as large as that for the nine O atoms of the first adlayer (see Table II). This adsorption energy difference seems to be due to the difference in the adsorption site, which will be discussed later.

TABLE II. Adsorption energies of each O adlayer on the Si surface.

Layer	Number of atoms in each layer	Adsorption energy (eV) per adlayer	per adatom
First	9	−74.6	−8.3
Second	9	−110.0	−12.2
Third	9	−75.7	−8.4

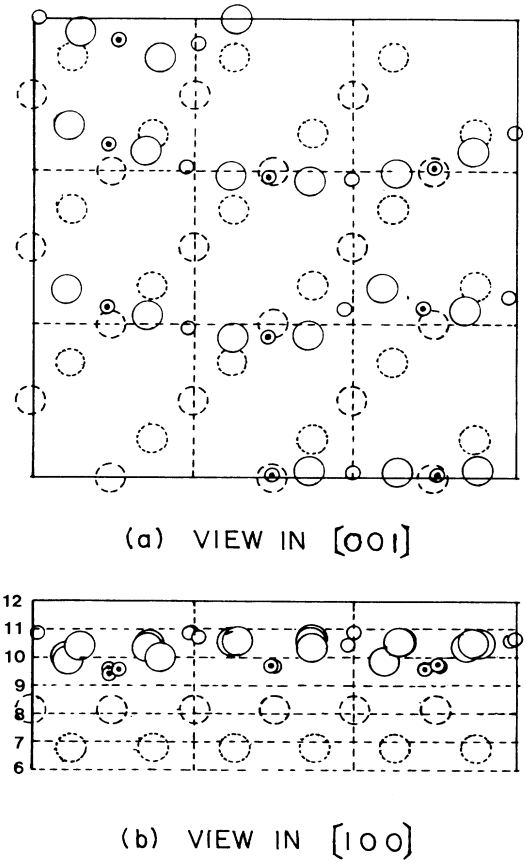

FIG. 2. The atomic arrangement for the first two O adlayers onto the Si(001) surface: (a) top view and (b) side view. Only the atoms of the top layer (solid-outlined circles) were allowed to relax for the Si substrate. ⊙ represents the atom of the second O adlayer.

The difference in bonding properties of Si and O atoms at the surface and in the bulk was checked by comparing bond angles and bond lengths for the case of 18 O adatoms. The average Si—O bond length decreased somewhat after the deposition of the second O adlayer (see Table III). The O—Si—O angles near the surface are distributed over 130°–170° and the average is about 150°, which is much larger than that for bulk SiO_2, (about 109°). The Si—O—Si angles are about 149° for the O atoms at the very surface (outward) and 122° for the O atoms on the second O layer (inward). For the Si—O—Si angle, the former is close to, but the latter is much smaller than, the Si—O—Si angle for bulk SiO_2 which is generally in the range of 144°–150°.

When nine O atoms of the third adlayer were deposited on the top of the Si surface, which had already adsorbed 18 O atoms, the third nine O adatoms occupied the other half of the *B*-type positions in Fig. 1(a) as shown in Figs. 3(a) and 3(b). Most of them went deeper than the O adatoms of the first and second adlayers and they were distributed over a range from positions 8–10. O adatoms de-

posited later tended to diffuse further into the Si lattice than those deposited earlier. This seems to be because the O atoms deposited earlier have already made with Si atoms bonds too strong for those deposited later to break. It was found that the adsorption depth of O atoms generally increased with the number of O adlayers or adatoms. Table III shows that the average Si—O—Si angle approaches that for the bulk SiO_2 (140°–150°) as the number of O adlayer increases.

Adsorption energy for the third Si adlayer is almost the same as that for the first adlayer. The reason why the adsorption energy for the second adlayer is about 1.5 times as great as those for the first and third adlayers is thought to be due to the difference in the adsorption site between atoms of different adlayers. The adsorption site for an atom of the third adlayer is of the same type as that for an atom of the first adlayer. After the adsorption of the second O adlayer the Si and O atoms were packed tightly in lines, which led to tight bonding between Si and O atoms in these lines and thus higher adsorption energy. However, after the third O adlayer was adsorbed, the bonding became loosened, since the O atoms of this new adlayer pulled Si atoms in the rows so that the atoms could distribute more uniformly.

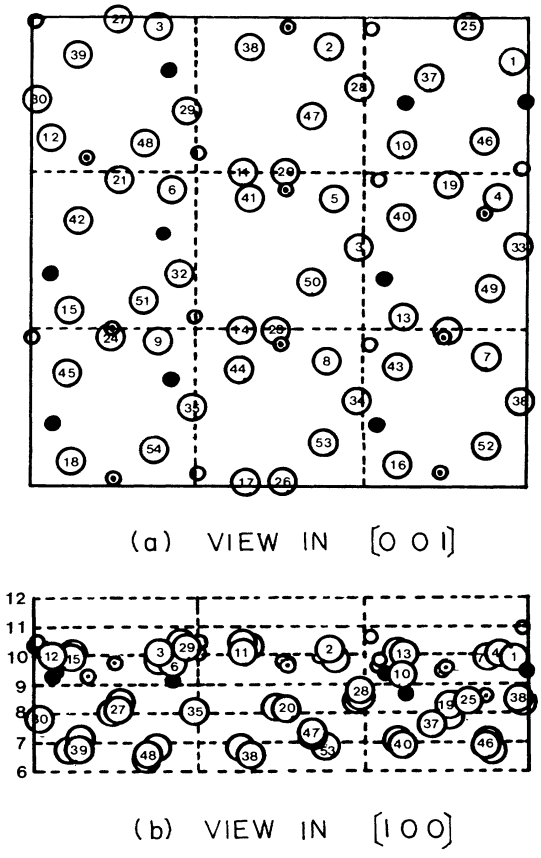

FIG. 3. The atomic arrangement for the first three O adlayers on the Si(001) surface: (a) top view and (b) side view. Atoms of the top three layers for the Si substrate which are numbered have been allowed to relax. Large and small circles represent Si and O atoms, respectively. ⊙ and ● represents the atoms of the second and third O adlayers, respectively. Numbers on the vertical axis in the side view denote heights in angstroms from the bottom of the Si substrate. The fixed part of the substrate is not shown in these figures.

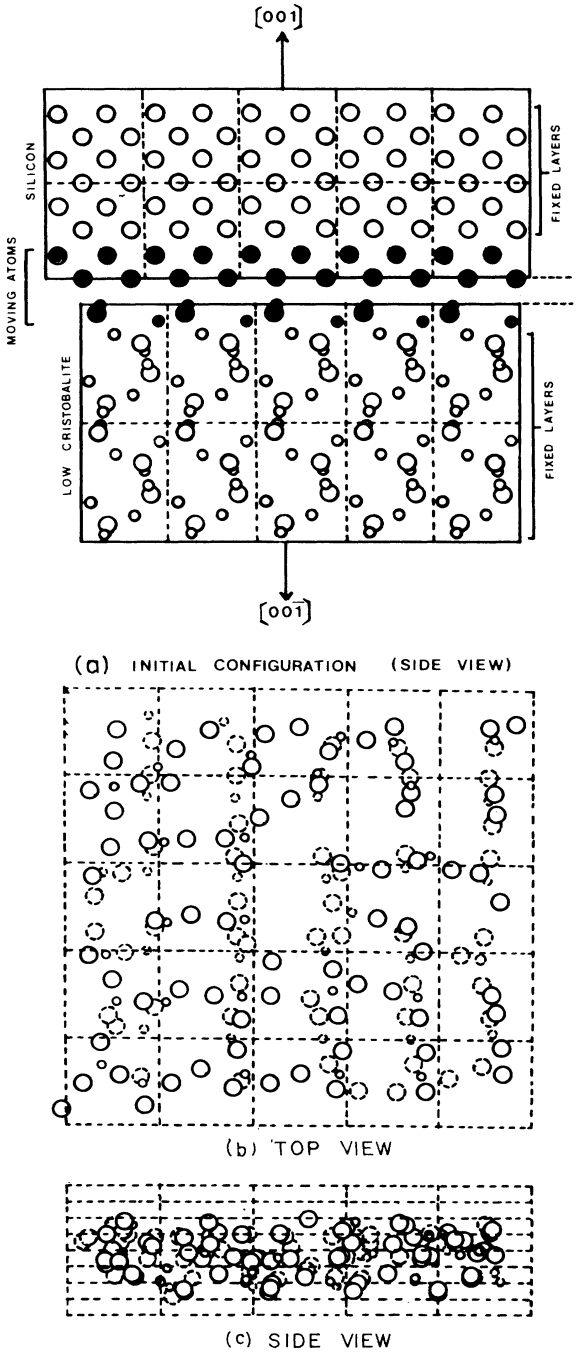

FIG. 4. Atomic configurations for the model system with the Si-SiO_2 interface: (a) Top view before relaxation. (Solid-outlined circles represent the atoms allowed to relax.) (b) Top view after relaxation. (c) Side view after relaxation. Only moving atoms are shown in (b) and (c). Dashed-outlined circles represent the 100 atoms located farther from the view point.

TABLE III. Structural data for the O adsorbed Si surfaces.

Layer	Total number of O adatoms	Si—O bond length (Å)	Si—O—Si angle	O—Si—O angle
1	9	1.60	163	
				149 (out)
2	18	1.56	150	122 (in)
3	27	1.57	147	135

C. The Si-SiO_2 interface

The model system employed in this run consists of perfect Si and low-cristobalite lattices. The size of each lattice is $5\times5\times2$ unit cells which is equivalent to 400 atoms for the former and 600 for the latter. The two lattices are joined by their (001) facing planes. This model differs from the previous ones mainly in that the Si and SiO_2 are placed together in their bulk form and that period boundary conditions are not imposed on the system. Thus, we have two surfaces on the (100) faces and two surfaces on the (010) faces of the sample cube and the regions near those surfaces must be excluded in considering structural change. The potential-energy cutoff radius in this simulation calculation was 5.0 Å. Simulation was performed at 1000 K.

In this simulation run only the atoms in the two layers (100 atoms) of the Si lattice and the three layers (75 atoms) of the SiO_2 lattice near the interface were allowed to relax. The initial atomic configuration in the near-Si-SiO_2 interface region is illustrated in Fig. 4(a). On the other hand, Figs. 4(b) and 4(c) show the atomic configuration after relaxation of the system at 1000 K.

We can see from these figures that the structure near the interface changes from ordered to disordered after equilibration, even if we start with crystalline forms for both the Si and SiO_2 parts. The structure of the SiO_x region is, in short, a transitional structure from Si to SiO_2. The nearest-neighbor distances between Si atoms are 2.352 and 3.077 Å in crystalline Si and low cristobalite, respectively, but those for the SiO_x region are distributed over a wide range, approximately from 2.2 to 3.2 Å, as shown in Fig. 5.

Grunthaner *et al.*[10] have reported an SiO_x region with a mixed composition comprising Si_2O_3, SiO and Si_2O as an x-ray photoemission spectroscopy result. According to the present simulation results, each O atom in the SiO_x region is surrounded by two, three, or four Si atoms. An O atom rarely forms bonds with only one Si atom or more than four Si atoms. The distribution of O atoms in terms of the number of Si atoms surrounding each O atom is given in Table IV. The case of an O atom coordinated by three Si atoms is predominant in the SiO_x region. A typical configuration of the Si_3O unit is a triangle of Si atoms with an O atom slightly above its center, although the degree of distortion for the triangle is variable. From Fig. 5 we can see that in comparison with the bulk SiO_2 region (the dashed line) the SiO_x region (the solid line) has a Si—Si bond distribution over a wider range, which implies that the distortion for the triangle is very irregular.

The average d(Si-O) is about 1.56 Å for the model with the separation between the Si and the SiO_2 of 1.20 Å. This value is slightly lower than that for crystalline SiO_2 which is about 1.68 Å. The shorter Si—O bond length indicates the high compressive stress in the Si-SiO_2 interface region.

Accuracy of a PEF is crucial in simulating the structure and properties of materials successfully. Yet it is very difficult to develop a PEF for the Si-O system, since the bonding properties of Si and O atoms are very per-

TABLE IV. Distribution of oxygen atoms in terms of the number of their neighboring silicon atoms (the cutoff Si—O bond length equals 2.0 Å). Total number of moving O atoms equals 40.

Number of Si atoms surrounding each O atom	Number of O atoms
1	1
2	14
3	23
4	11
5	1

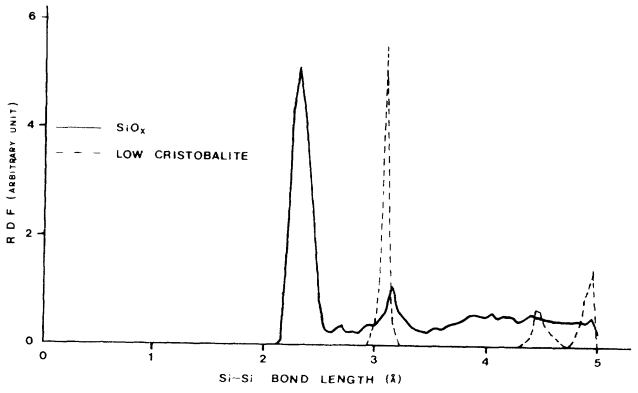

FIG. 5. Radial distribution functions of the Si—Si bond length: The solid curve is for the model system in the Figs. 4(b) and 4(c). The dashed curve is for a crystalline silica.

plexing. Moreover, it is next to impossible to establish a PEF with a simple form which can reflect their bonding properties accurately especially near their surfaces and interfaces. This work, in this respect, may be regarded as an attempt at simulating Si thermal oxidation. Therefore, reported numerical results may be only semiqualitative in nature, and should be treated accordingly. For more accurate quantitative results fine tuning of parameters in the PEF would be necessary.

IV. SUMMARY AND CONCLUSIONS

In the preceding section we discussed the structure and energy-related properties for a clean Si surface, O-adsorbed Si surfaces, and a Si-SiO_2 interface. A brief summary of these simulation results follows.

A. The clean Si surface

The reconstructed Si(001) surface exhibits the formation of dimers alternately throughout the surface.

B. O adsorption on the Si surface

(1) Energetically the most favorable position of an O adatom on the Si(100) surface is slightly above the center of two Si atoms which approach each other by relaxation on the clean Si surface; the binding energy of a single O adatom to the Si lattice is -8.4 eV. Also the Si—O bond length and Si—O—Si angle for chemisorption of an O atom on the Si(100) 1×1 surface are 1.60 Å and 163°, respectively.

(2) The O atoms in adlayers deposited later move deeper into the Si substrate than atoms from previously deposited adlayers.

(3) The binding energy of the O atoms for subsequent adlayers is larger than that for the initial adlayers. The binding energy for each of the three O adlayers is summarized in Table II.

(4) The adsorption depth of O atoms increases with the number of O adlayers or adatoms.

(5) The average Si—O bond length, Si—O—Si and O—Si—O bond angles at this surface after the deposition of the third O adlayer are average Si—O bond length of 1.57 Å, average Si—O—Si bond angle of 147°, and average O—Si—O bond angle of 135°. The angles are distributed over a wide range. The O—Si—O bond angle at this surface is considerably larger than that in bulk SiO_2.

C. The Si-SiO_2 interface

(1) The nonstoichiometric (SiO_x) region is formed mostly by the diffusion of O atoms.

(2) The predominant bonding unit in the SiO_x region is Si_3O, and its typical configuration is a triangle of Si atoms with the O atom slightly above its center.

(3) The average Si—O bond length is 1.56 Å, which is somewhat smaller than that in the crystalline SiO_2 (1.60 Å).

ACKNOWLEDGMENTS

The author would like to thank Professor W. A. Tiller of Stanford University and Dr. Timur Halicioglu of NASA Ames Research Center (Moffett Field, CA) for their many helpful discussions and useful suggestions. He is also grateful to the NASA Ames Research Center for a generous allocation of computer time.

[1]See, for example, F. Meyer and M. J. Sparmany, in *Surface Physics of Phosphors and Semiconductors*, edited by C. G. Scott and C. E. Reed (Academic, New York, 1975), p. 321; H. Ibach, K. Horn, R. Dorn, and H. Luth, Surf. Sci. **38**, 433 (1973).

[2]A. Redondo, W. A. Goddard III, C. A. Swarts, and T. C. McGill, J. Vac. Sci. Technol. **19**, 498 (1981).

[3]C. Lee, J. Phys. C **19**, 5555 (1986).

[4]C. Lee, J. Korean Ceram. Soc. **23**, 47 (1986).

[5]C. Lee, Phys. Status Solidi B **139**, K93 (1987).

[6]T. Halicioglu, Phys. Status Solidi B **99**, 347 (1980).

[7]T. Takai, T. Halicioglu, and W. A. Tiller, Phys. Status Solidi B **130**, 131 (1985).

[8]D. E. Eastman, J. Vac. Sci. Technol. **17**, 492 (1980).

[9]W. Monch, Surf. Sci. **86**, 672 (1979).

[10]I. P. Batra, P. S. Bagus, and K. Hermann, J. Vac. Sci. Technol. A **2**, 1075 (1984).

[11]J. A. Schaefer, F. Stucki, D. J. Frankel, W. Gopel, and G. J. Lapeyre, J. Vac. Sci. Technol. B **2**, 359 (1984).

[12]C. Y. Su, P. R. Skeath, I. Lindau, and W. E. Spicer, J. Vac. Sci. Technol. **18**, 843 (1981).

[13]G. Hollinger and F. J. Himpsel, J. Vac. Sci. Technol. A **1**, 640 (1983).

[14]F. J. Grunthaner, B. F. Lewis, J. Maserjian, and A. Madhukar, J. Vac. Sci. Technol. **20**, 747 (1982).